



LAWRENCE
LIVERMORE
NATIONAL
LABORATORY

RESPONSE OF ALUMINUM SPHERES IN SITU TO DETONATION

J.D. Molitoris, R. G. Garza, J. W. Tringe, J. D. Batteux,
B. M. Wong, R. J. Villafana, B. A. Cracchiola, J. W.
Forbes

April 12, 2010

14th International Detonation Symposium
Coeur d'Alene , ID, United States
April 11, 2010 through April 16, 2010

Disclaimer

This document was prepared as an account of work sponsored by an agency of the United States government. Neither the United States government nor Lawrence Livermore National Security, LLC, nor any of their employees makes any warranty, expressed or implied, or assumes any legal liability or responsibility for the accuracy, completeness, or usefulness of any information, apparatus, product, or process disclosed, or represents that its use would not infringe privately owned rights. Reference herein to any specific commercial product, process, or service by trade name, trademark, manufacturer, or otherwise does not necessarily constitute or imply its endorsement, recommendation, or favoring by the United States government or Lawrence Livermore National Security, LLC. The views and opinions of authors expressed herein do not necessarily state or reflect those of the United States government or Lawrence Livermore National Security, LLC, and shall not be used for advertising or product endorsement purposes.

Response of Aluminum Spheres In Situ to Detonation

J. D. Molitoris, R. G. Garza, J. W. Tringe, J. D. Batteux , B. M. Wong,
R. J. Villafana, B. A. Cracchiola and J. W. Forbes*
Energetic Materials Center, Lawrence Livermore National Laboratory, Livermore, CA 94550
**Energetics Technology Center, La Plata, MD 20646*

Abstract

Time sequence x-ray imaging was utilized to determine the response of aluminum spheres embedded in a detonating high-explosive cylinder. The size of these spheres ranged from 3/8" to 1/32" in diameter. These experiments directly observed the response of the spheres as a function of time after interaction with the detonation wave. As the spheres are entrained in the post-detonation flow field, they are accelerating and their velocity profile is complicated, but can be determined from the radiography. Using the aluminum spheres as tracers, radial velocities of order 1.6 mm/us and horizontal velocities of order 0.08 mm/us were measured at early times post detonation. In terms of response, these data show that the largest sphere deforms and fractures post detonation. The intermediate size spheres suffer negligible deformation, but appear to ablate post detonation. Post detonation, the smallest spheres either react, mechanically disintegrate, atomize as a liquid or some combination of these.

Introduction

Time controlled application of thermal and mechanical energy is highly advantageous for enhanced blast and blast applications. However, the interaction of solid fuels like aluminum with explosives is not well-understood for a wide range of scenarios of interest. For example, thermo-chemical codes like Cheetah are effective for determining the final fate of materials following an explosive event, but it is always assumed that the materials and explosives are homogeneous distributed. In reality, solid fuel-containing bodies can remain intact and un-reacted for extended periods, and the mechanical and chemical energy retained by these bodies as a function of time is critical for optimizing the functionality of the weapons system. Here we perform detailed x-ray imaging experiments to directly observe the fate of aluminum spheres immediately following shock loading by detonation.

Test Article Fabrication

Two types of parts were made: a wax fiducial to aid in experimental design, and a high-explosive test article. In total there were two fiducials and two test articles constructed. For the first half of the explosive test article, the target and actual weights of explosive and other functional materials are given in Table 1.

Table 1: Material weights for Formulation 1, first half of fiducial article casting

Material	Wt %	Weight (g)	Actual Wt. (g)
LX-20 (RX-08-HD)	99.2	63.49	30.26+ 33.23 = 63.49
Dabco 131 catalyst	0.001 - 0.008	0.005	0.0049
Desmodur N-100	0.8	0.51	0.52
Total	100.0	64.0	64.0

For the first fill, the Cramer mixer and de-aerator loader were used. The article was filled most of the way before running out of LX-20, then topped off with material from lines of the de-aerator/loader. The plate on the molds had to be removed while the LX-20 was uncured to place the aluminum spheres.

Spheres were inserted ~2 hours after the crosslinker was added. Aluminum spheres were inserted by eye according to the schematic shown in Fig. 1. Tweezers were used to push spheres until covered to half diameter in LX-20. Aluminum spheres with diameters of 1/32" (4 spheres), 5/64" (3 spheres), 3/32" (3 spheres), 1/8" (1 sphere) and 3/8" (1 sphere) were used.

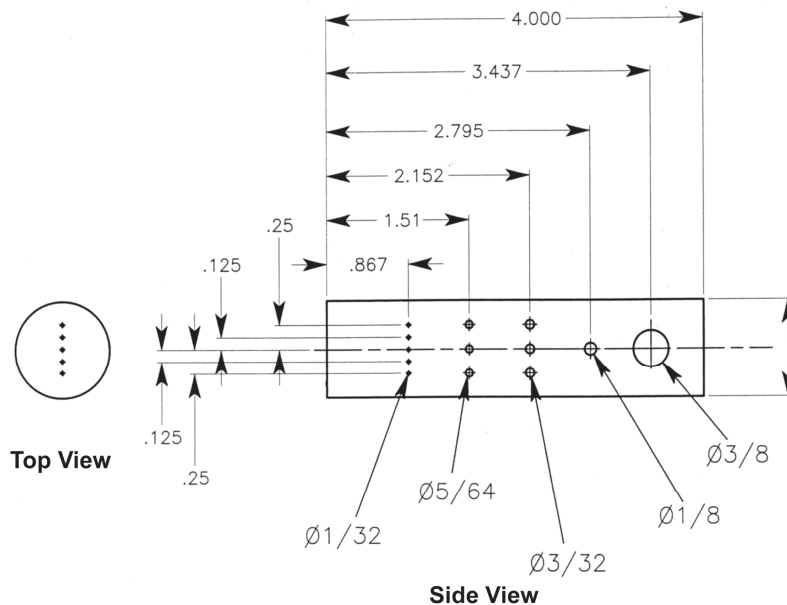


Figure 1. Schematic of sphere placement in test article.

The cured half-structure is shown in Fig. 2 below.

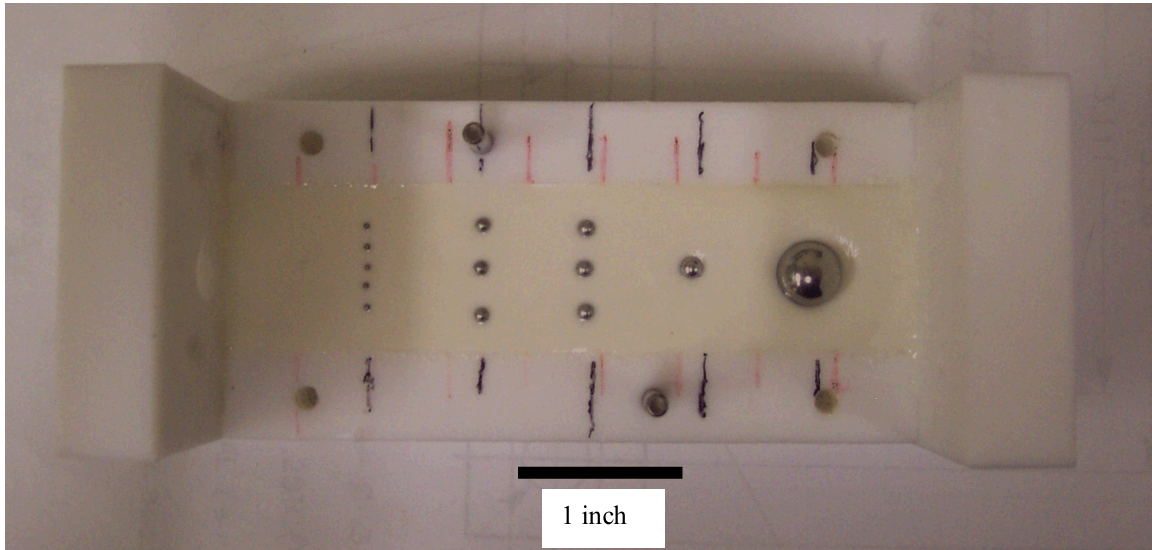


Figure 2. LX-20 half structure with aluminum spheres in shot set-up

For the second half of the test article, the target and actual weights of explosive and other functional materials are given in Table 2 below.

Table 2: Material weights for Formulation 2, second half of test article casting

Material	Wt %	Weight (g)	Actual Wt. (g)
LX-20 (RX-08-HD)	99.2	63.41	50.30+ 14.11 = 64.41
Dabco 131 catalyst	0.001 - 0.008	0.005	0.005
Desmodur N-100	0.8	0.51	0.529
Total	100.0	64.0	64.94

The completed article showed good uniformity throughout as verified by radiography, Fig. 3. Fig. 3 also shows the initiator and holder mechanisms employed during the shot itself.

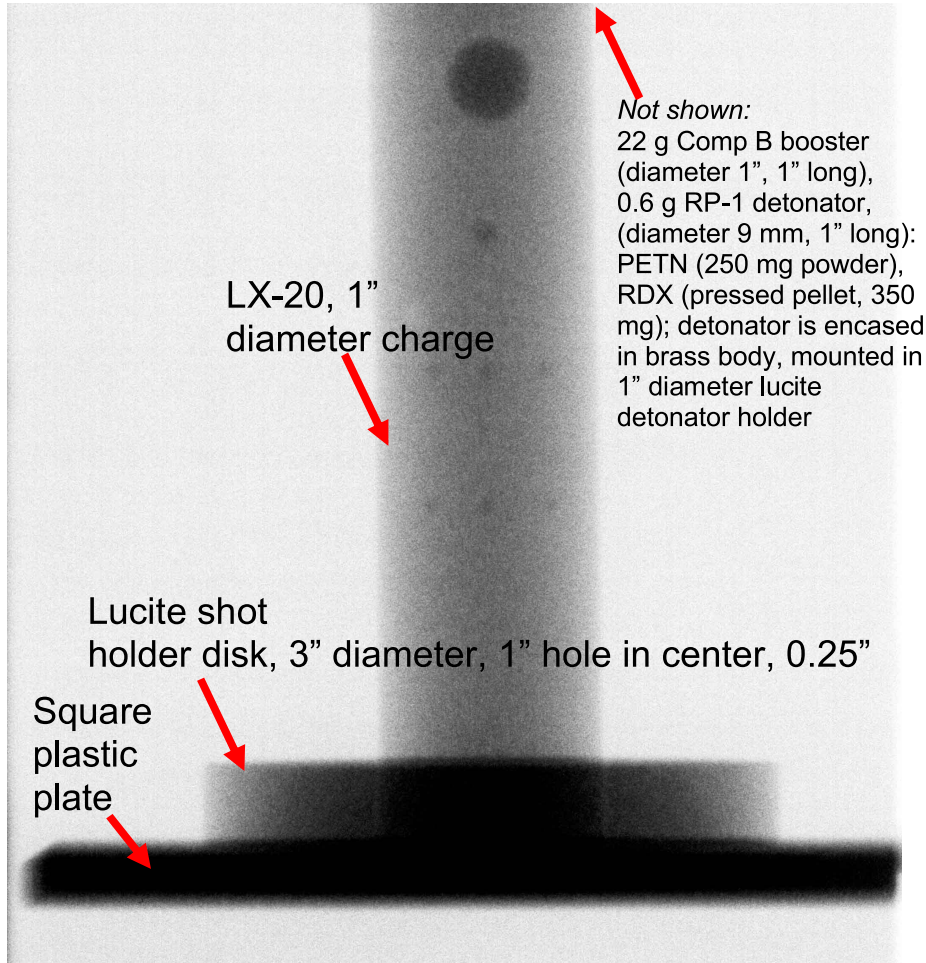


Figure 3. Completed test article showing LX-20 uniformity, also initiation and holder mechanisms.

Experimental results

Experiments were performed in the LLNL High Explosives Application Facility's 10 kg spherical tank, with the Hydra x-ray imaging system. In this system, three independent x-ray heads were aligned around the cylindrically-symmetric target, as shown in Fig. 4.

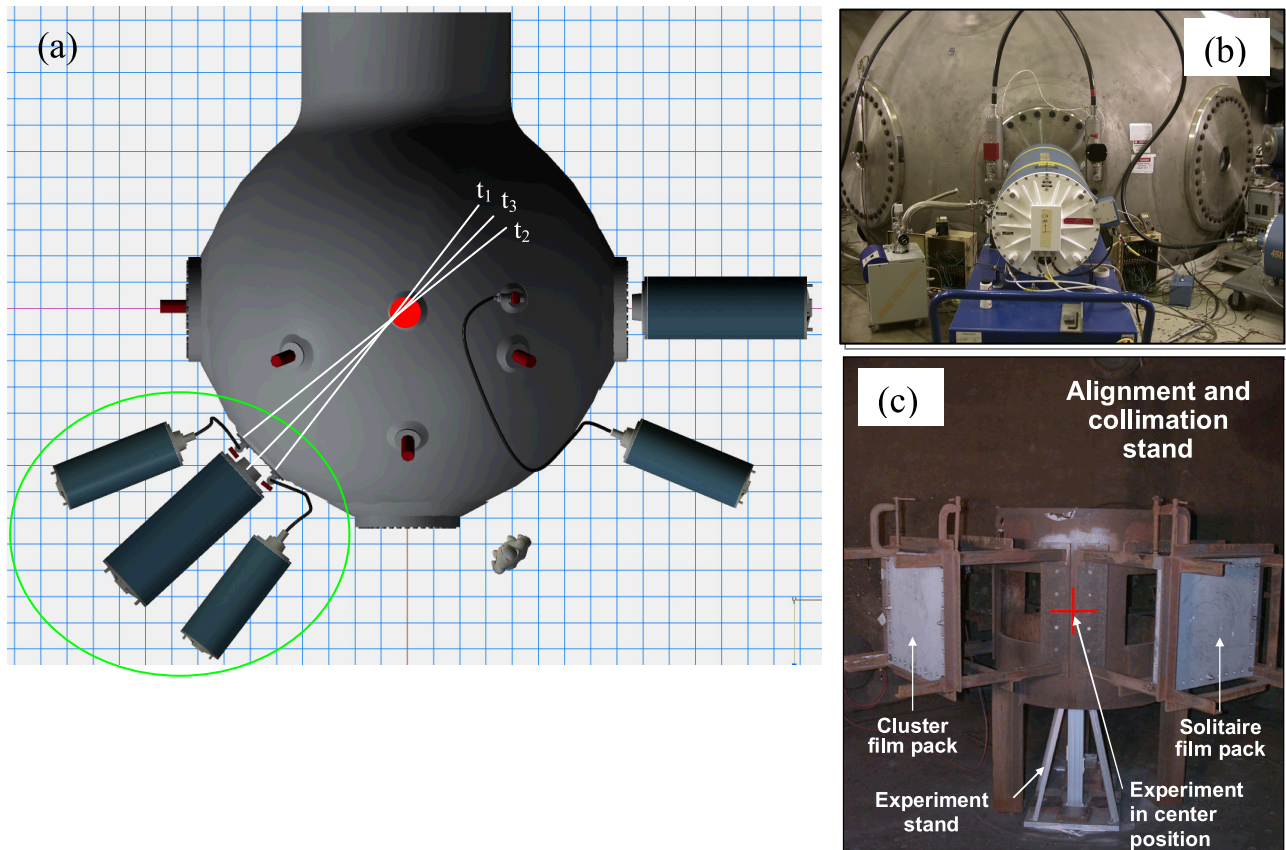


Figure 4. (a) Top-down view of Hydra flash x-ray system. The capacitor banks which generate the current pulses which drive the x-ray pulses are shown as cylinders surrounding the spherical 10-kg tank, with a top-down view of a person for scale. The three x-ray elements used for this experiment are circled in green. They were flashed in series to create images at t_1 , t_2 and t_3 . (b) Photograph of the tank and x-ray generators. (c) View of target stand and film.

The x-rays were designed to flash in sequence to characterize the evolution of the explosive and spheres as a function of time.

As described previously, two nominally identical cylindrical LX-20 test article were fabricated, each with 12 spheres of varying diameters: $1/32''$ (4 spheres), $5/64''$ (3 spheres), $3/32''$ (3 spheres), $1/8''$ (1 sphere) and $3/8''$ (1 sphere). One article was initiated such that the largest sphere was shocked first, and the second was initiated such that the largest sphere was shocked last as shown in Figs. 5 and 6.

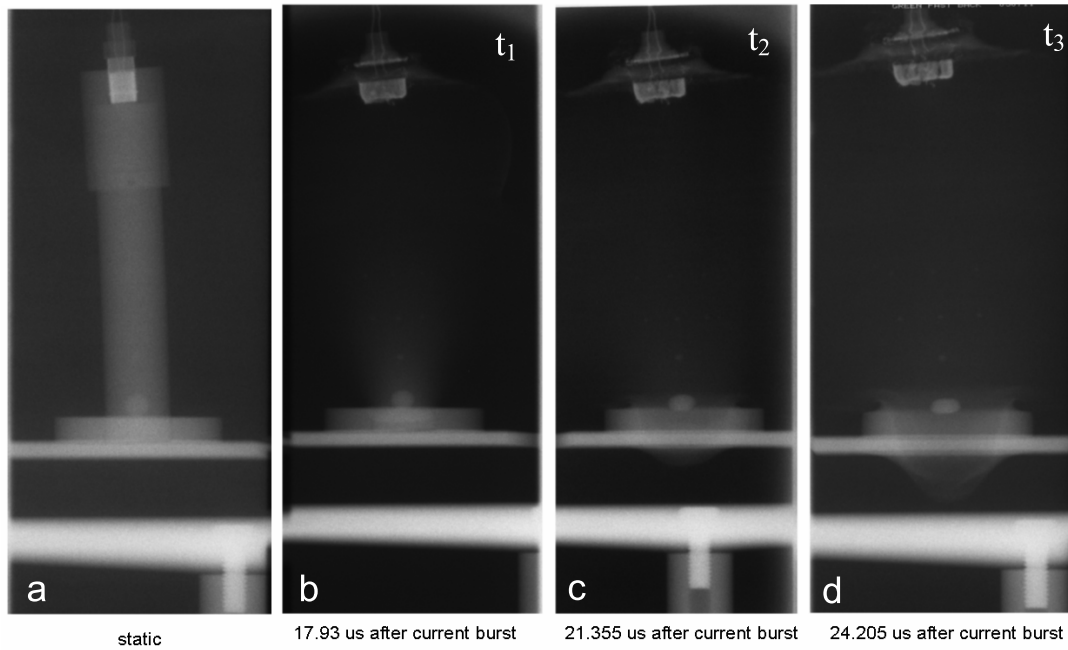


Figure 5. Cylindrical LX-20 test article, 1inch in diameter, filled with aluminum spheres of varying diameter; initiated such that largest sphere is shocked last. Time sequence of images are labeled.

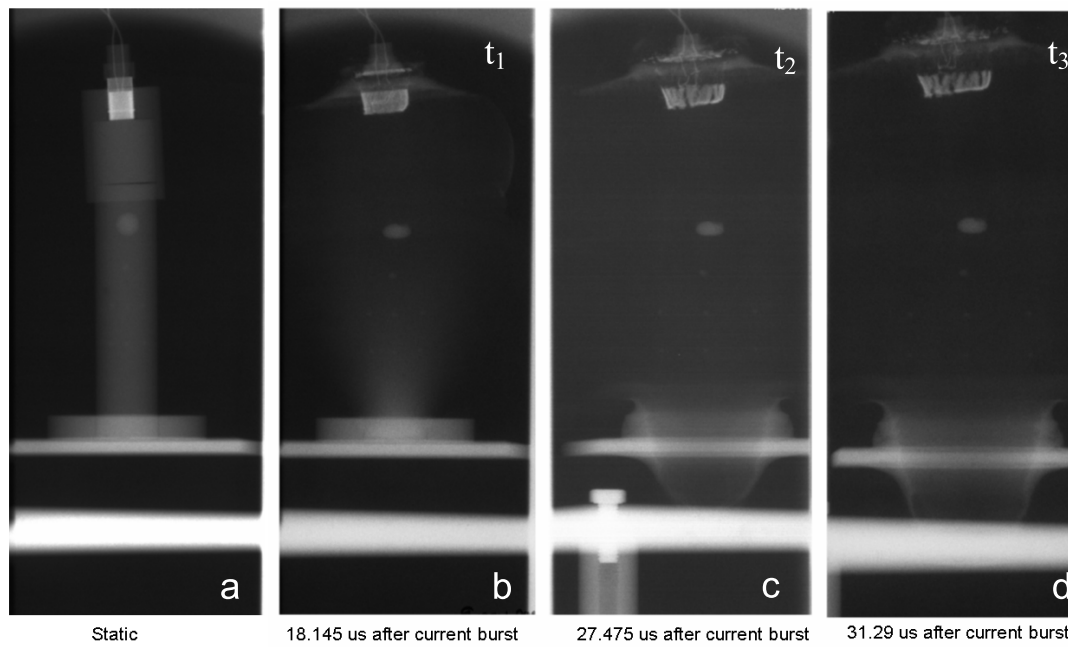


Figure 6. Cylindrical LX-20 test article, 1inch in diameter, filled with aluminum spheres of varying diameter; initiated such that largest sphere is shocked first. Time sequence of images are labeled.

Discussion

In Fig. 5(a), the large sphere at the bottom of the 4" LX-20 cylinder has been impacted at time $17.9 \mu\text{s}$ after current burst. This implies shock velocity in excess of 5.7 km/s , which is larger than expected for pure LX-20 by more than a factor of 2. We hypothesize that the shock has been accelerated by the more dense aluminum.

A more detailed analysis of the sphere dynamics from Fig. 6 is shown in Figs. 7 and 8. Here we observe smaller spheres moving radially and away from the initiation point at velocities of several hundred m/s.

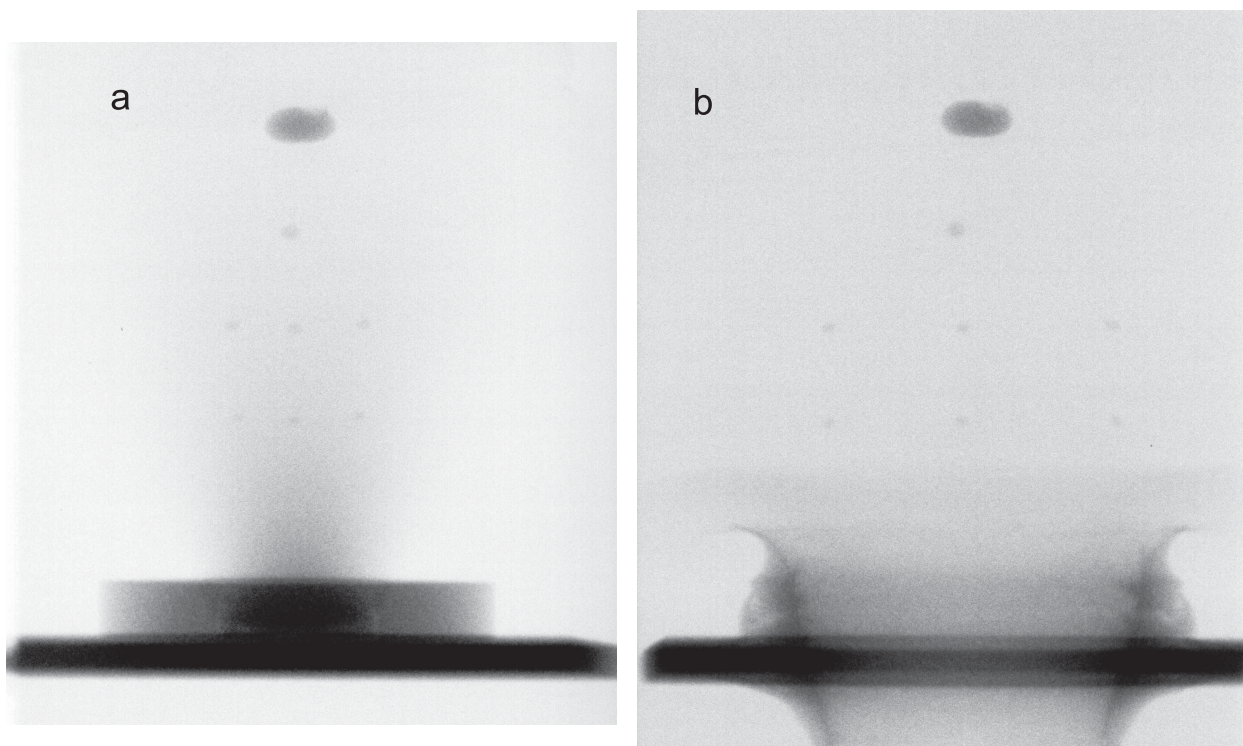


Figure 7. Detailed analysis of sphere dynamics during post-detonation. Images (a) and (b) are separated by $13.1 \mu\text{s}$.

Once the detonation has reduced the solid HE to expanding reaction products, the spheres are clearly visible. Their separation can be used to track the flow of the reaction products, but our interest here is in changes in their size and shape due to detonation. Only the largest sphere ($0.375''$) suffers significant deformation and cracking. Fig. 8 shows an expanded view.

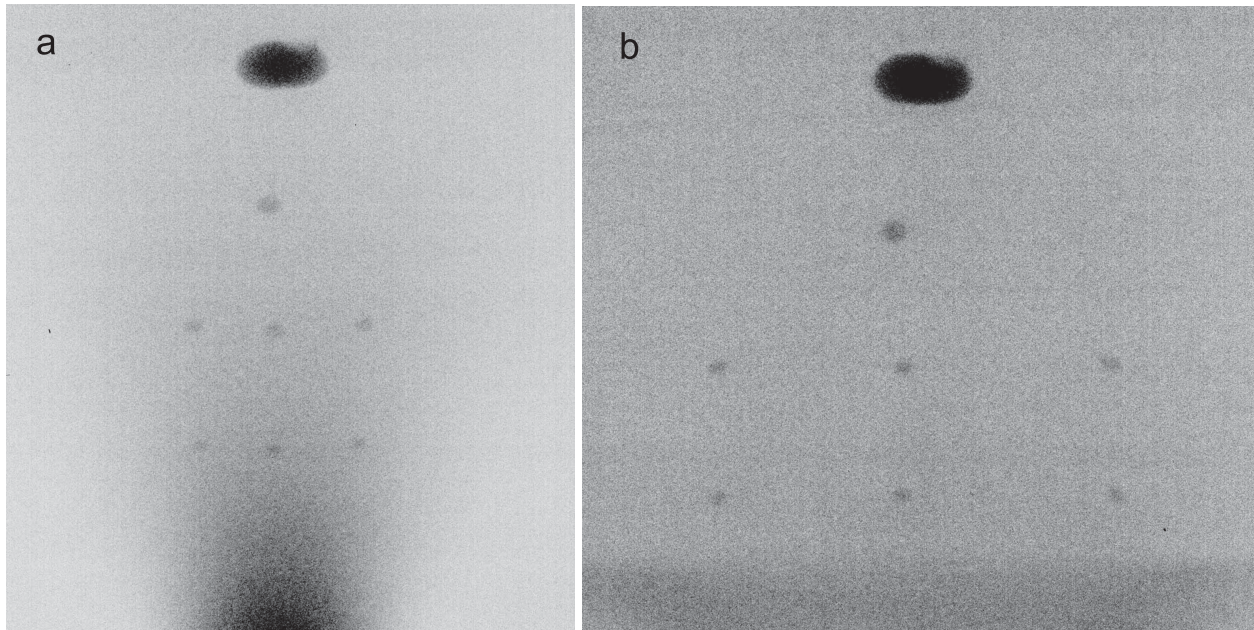


Figure 8. Expanded image from Fig. 7. The two images are properly spatially scaled so they are directly comparable. Images (a) and (b) are separated by 13.1 μs .

The smallest spheres should be visible with no solid high explosive, but they are not. Instead, there is a dark band in this image where the smallest spheres (0.03") should be, suggesting spheres have reacted or ablated. The intermediate spheres (0.125", 0.094" and 0.08"), by contrast, are easily tracked and analyzed.

A more detailed analysis of the sphere dynamics from Fig. 5 is shown in Fig 9. As before, we observe small spheres moving radially and away from the initiation point at velocities of several hundred m/s.

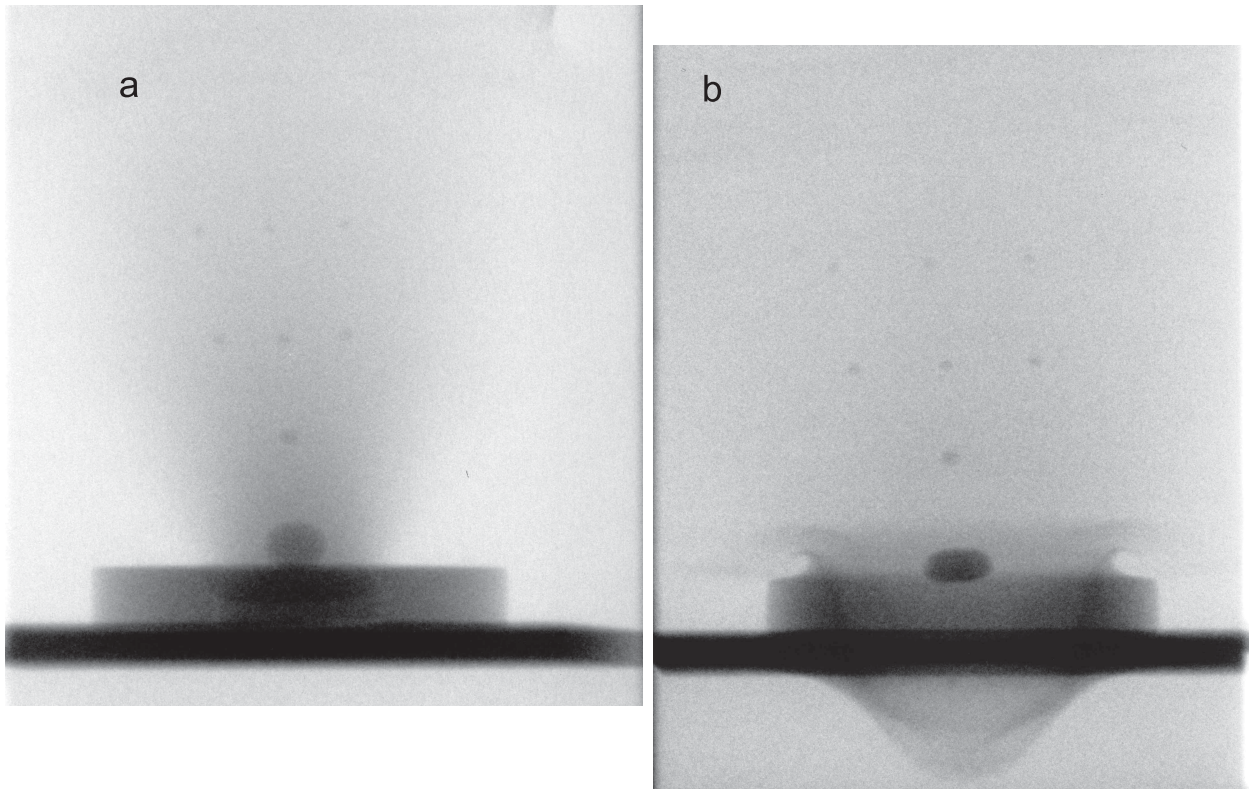


Figure 8. Expanded image from Fig. 7. Images (a) and (b) are separated by 6.3 μ s.

The smallest spheres are not visible in this experiment either, indicating that obscuration of these spheres by the ablated target stand in the experiment shown in Fig. 8 may not have been an issue. However, the dark band previously visible is no longer present.

Based on this data, we can draw some preliminary conclusions. Intermediate spheres (0.125", 0.094" and 0.078" diameter), stay roughly spherical after detonation, and do not break up. Diameters are reduced smoothly as a function of time. The largest sphere (0.375" diameter), by contrast, exhibits significant deformation and possible surface ablation. The smallest spheres, (0.031" diameter) should be discernible in the post-detonation data, but are not. They are either beyond the resolution limit of our x-ray system, or are atomized by the detonation.

Flow field velocity determination post-detonation

As the aluminum spheres had a relatively high contrast, it is straight-forward to track their motion and determine their radial and in-line velocity from the time sequence x-ray images. The outer 3/32 and 5/64 inch diameter spheres had measured radial velocities of order 1.6 mm/us and in-line (with the detonation direction) velocities that were much slower, about 0.08 mm/us. The two velocity components also varied with the mass/size of the sphere. The larger spheres moved slower and the smaller spheres moved faster in the post-detonation flow field. The measured velocity also increased with time. As the aluminum spheres were lighter than available higher contrast materials (ie. tungsten, tungsten carbide, of tantalum) they followed the flow field

closely, but had the disadvantage of being reactive and effected by the violence and intense heat. We are in the process of attempting to map the post-detonation flow field from these data.

Summary

For 0.375"-0.078" spherical particles, aluminum consumed in detonation is minimal as there is no large size reduction of the particles. This may optimize the aluminum available for post-detonation combustion, leading to an enhanced blast effect greater than the smaller particles typically mixed into high-explosive. For this reason, it is of great interest to determine if spheres of about 0.031" diameter are atomized and possibly utilized by the detonation.

Acknowledgements

We acknowledge the partial support of the Advanced Energetics Program, Defense Threat Reduction Agency for these experiments. This work was performed under the auspices of the U.S. Dept. of Energy Lawrence Livermore National Laboratory under Contract DE-AC52-07NA27344.